

# Breakup Threshold Anomaly: New Manifestation of the Dispersion Relation.

L. C. Chamon<sup>1</sup>, P. R. S. Gomes<sup>2</sup> and M. S. Hussein<sup>1</sup>.

<sup>1</sup>*Instituto de Física da Universidade de São Paulo,  
Caixa Postal 66318, 05315-970, São Paulo, SP, Brazil.*

<sup>2</sup>*Instituto de Física, Universidade Federal Fluminense,  
Av. Litoranea s/n, Gragoatá, Niterói, RJ, Brazil, 24210-340.*

(Dated: August 4, 2019)

It is pointed out that the usual threshold anomaly, found operative in the energy behavior of the imaginary and real parts of the optical potential representing the elastic scattering of tightly bound nuclei at near- and below-barrier energies, suffers a drastic qualitative change in the case of the elastic scattering of weakly bound projectile nuclei. Owing to the strong coupling to the breakup channel even at sub-barrier energies, the imaginary potential strength seems to increase as the energy is lowered down to below the natural, barrier, threshold, accompanied by a decrease in the real potential strength. This feature is consistent with the dispersion relation. It also clearly indicates the effective increase of the barrier height. The systems  ${}^9\text{Be}$ ,  ${}^{16}\text{O} + {}^{64}\text{Zn}$  and  ${}^{6,7}\text{Li} + {}^{138}\text{Ba}$  are analyzed to illustrate this new phenomenon.

PACS numbers: 25.70.Bc, 25.70.Mn

The, by now, well known Threshold Anomaly (TA), seen in the behavior of the real and imaginary parts of the optical potential as a function of decreasing energy in the elastic scattering of tightly bound nuclei at near-barrier energies, has been reviewed and discussed by several authors [1, 2]. The phenomenon is a direct consequence of the dispersion relation which quantifies the concept of causality in scattering: no scattered wave emerges before the incident wave reaches the target. Recently, the TA has been looked for in the case of the elastic scattering of weakly bound stable and radioactive nuclei [3, 4, 5]. It has been suggested that the TA "vanishes" for such systems. However, careful analyses of the data show that what happens in these systems is a new manifestation of the dispersion relation unique for breakup coupling dynamical polarization potential. Because the coupling to the breakup in these systems continues to be important even at energies below the barrier, the "threshold" ceases to be the barrier itself. Thus, the imaginary part of the potential could increase at lower energies and, as the dispersion relation dictates, the real part of the dynamic potential would show a decrease, implying an overall decrease in the real part of the optical potential that fits the elastic scattering. This is indeed what is found [4, 5]. The purpose of this letter is to give a detailed account of this phenomenon, which we coin as the Breakup Threshold Anomaly (BTA).

We first present the analyses for the "normal" system  ${}^{16}\text{O} + {}^{64}\text{Zn}$ , where elastic scattering angular distributions at several energies have been measured [6]. We have re-analyzed the data using the São Paulo (SP) optical potential. The SP interaction [7, 8, 9, 10] is based on the double folding potential with account to exchange through an effective energy dependence:

$$V_{SP}(R, E) = (1 + i 0.78) F(R, E), \quad (1)$$

where  $F(R, E)$  is the double folding potential whose energy dependence results from the local equivalence of the

otherwise non-local interaction [11, 12]. This energy dependence is not dispersive. In the present analysis, we have assumed for the optical potential a normalized version of the SP potential:

$$V_{SP}(R, E) = [N_R(E) + iN_I(E)] F(R, E). \quad (2)$$

The coefficients  $N_R(E)$  and  $N_I(E)$  are energy dependent normalization factors that take into account the effects of the dynamic polarization potentials (DPP) arising from direct channel couplings. It is worth mentioning here that all DPPs are dispersive with their real and imaginary parts being connected through a dispersion relation. One important exception to this is the elastic transfer DPP [13].

From the properties of the Green function, that enters in the definition of the DPP, one can immediately derive the dispersion relation between  $N_R(E)$  and  $N_I(E)$ , represented by:

$$N_R(E) = N_{R0} + \Delta N_R(E), \quad (3)$$

$$\Delta N_R(E) = \frac{P}{\pi} \int \frac{N_I(E')}{E' - E} dE'. \quad (4)$$

These equations are the analog of the Kramer-Kronig dispersion relation in optics, and arise from general principle of causality: no scattered wave emerges before the incident wave reaches the scattering center.

In figure 1, we show the behavior of  $N_R(E)$  and  $N_I(E)$  obtained from elastic scattering data fits for the normal system mentioned above. Because the threshold for non-elastic channel coupling effects is the Coulomb barrier, one observes the TA as expected: a decrease in  $N_I(E)$  as the energy is lowered below the barrier, accompanied by an increase in  $N_R(E)$ , implying an increase in the attraction and accordingly a reduction of the barrier height. This favors an enhancement in the complete fusion cross

section as has been demonstrated for a wide range of systems involving normal, tightly bound nuclear projectiles [15]. Just to illustrate the dispersion relation, we have assumed a schematic description for  $N_I$

$$N_I = 0 \text{ for } E \leq E_1, \quad (5)$$

$$N_I = a(E - E_1) \text{ for } E_1 \leq E \leq E_2, \quad (6)$$

$$N_I = a(E_2 - E_1) + b(E - E_2) \text{ for } E_2 \leq E \leq E_3, \quad (7)$$

$$N_I = a(E_2 - E_1) + b(E_3 - E_2) = N_{I\infty} \text{ for } E \geq E_3. \quad (8)$$

Within this assumption, one obtains an analytical expression for  $\Delta N_R$  [1, 2]

$$\begin{aligned} \Delta N_R(E) = & a(E_2 - E_1) [\epsilon_1 \ln|\epsilon_1| - \epsilon_2 \ln|\epsilon_2|] \quad (9) \\ & + [b(E_3 - E_2) - a(E_2 - E_1)] \\ & \times [\epsilon'_2 \ln|\epsilon'_2| - \epsilon'_3 \ln|\epsilon'_3|], \end{aligned}$$

with  $\epsilon_i = (E - E_i)/(E_2 - E_1)$  and  $\epsilon'_i = (E - E_i)/(E_3 - E_2)$ . The solid lines in figure 1 represent a behavior of  $N_R(E)$  and  $N_I(E)$  within this schematic picture. The elastic scattering angular distribution for the lowest energy of the  $^{16}\text{O} + ^{64}\text{Zn}$  system is presented in the inset of Fig. (1). The dashed line in this inset represents predictions obtained with the standard values  $N_R=1$  and  $N_I=0.78$ , while the solid line corresponds to the results obtained with the best  $N_R$  and  $N_I$  values for this energy. A comparison between these dashed and solid lines shows that the data fit is quite sensitive to the  $N_R$  and  $N_I$  values even at this low energy region.

We turn now to the weakly bound nucleus  $^9\text{Be}$  and study its elastic scattering on the same target  $^{64}\text{Zn}$ . We have re-analyzed elastic scattering angular distributions at several bombarding energies [4]. The corresponding  $N_R(E)$  and  $N_I(E)$  are shown in figure 2. A striking difference in the energy dependence of these normalization coefficients from the one shown in the previous figure (figure 1) is clearly seen. As the energy is lowered below the barrier  $N_R(E)$  decreases, while  $N_I(E)$  increases. This implies an effective reduction of the nuclear attraction leading to an increase in the barrier height. Accordingly, the complete fusion cross section may be hindered in comparison with the opposite results expected for tightly bound stable nuclei, giving more credence to the findings of several authors in theory [16, 17, 18] and experiment [19, 20, 21, 22]. The solid lines in figure 2 represent behaviors of  $N_R$  and  $N_I$  that are compatible with the dispersion relation. We have also performed similar re-analyses for the  $^6,7\text{Li} + ^{138}\text{Ba}$  systems (elastic scattering data from Ref. [23]). The corresponding results (see Figs. 3 and 4) are very similar to those for  $^9\text{Be} + ^{64}\text{Zn}$ .

It seems therefore that the threshold for non elastic processes of these systems is several MeV below the barrier, as the solid lines in figures (2)-(4) indicate, in agreement with the schematic calculations of Ref. [17].

A further evidence of the consistence of our analyses are the values obtained for  $N_{R0}$  and  $N_{I\infty}$ . As the SP potential, equation (1), has been successful in describing the elastic scattering for a large number of different systems in energies above the barrier [10], one should expect that both  $N_{R0}$  and  $N_{I\infty}$  to be close to unity. Of course, the values for  $N_{R0}$  and  $N_{I\infty}$  found in the present work are not identical to the standard (from high energies)  $N_R=1$  and  $N_I=0.78$ . However, these standard values in fact represent mean values obtained from data analyses of several systems [10] and one can expect variations around the average values for particular systems. Indeed, structure effects on the nuclear densities involved in the folding calculations may affect  $N_R$  while different degrees of absorption from particular reaction channels could affect  $N_I$ . An inspection of Figs. 1-4 shows that  $0.9 \leq N_{R0} \leq 1.15$  and  $0.5 < N_{I\infty} < 1.5$  have been found in the present work.

As already commented, the solid lines in Figs. 1-4 represent behaviors of  $N_R$  and  $N_I$  compatibles with the dispersion relation. In fact, different behaviors, that also could follow the "data", can be found even within the schematic picture of Eqs. 5-7 just by slightly modifying the values of the parameters involved in these equations. Therefore, clearly our findings are mainly based on the  $N_R$  and  $N_I$  "data" themselves. The detected difference between the normal and weakly-bound systems is mostly based on the results from the corresponding lowest energies (see Figs. 1-4). Even so, we consider that significant evidence for the proposed BTA has been obtained, because the data fits for these low energies are still quite sensitive to  $N_R$  and  $N_I$ , as illustrated by the dashed and solid lines in the insets of Figs. 1-4.

Traditionally, the threshold anomaly is formally displayed in terms of complex renormalization factors of the double-folding potential, as we have done in the present work. This assumption, which corresponds to assume that the radial dependence of the optical potential is the same as the bare one, is well established for normal tightly bound stable nucleus systems. The situation is more complicated in the case of weakly bound nuclei, where the effect of the couplings give rise to a polarization potential with different radial shape. In particular, an important role is played by the tail of the polarization which is much longer than that of the folding potential [24]. Nevertheless, our simple approach of considering renormalization factors has provided good fits, not only for the data shown in the insets of figures 1-4, but for all angular distributions analyzed in the present work

In conclusion, we have found some evidence of differences in the energy-dependence of the optical potential for tightly and weakly bound nucleus systems. The Break-up Threshold Anomaly implies an increase of the imaginary part and a decrease of the real part of the

optical potential that fits the elastic scattering at low energies. This reduction in the attraction results in an increase of the barrier height. Consequently, a possible hindrance in the complete fusion may erase any enhancement due to the larger size of the weakly bound nucleus. In fact this behavior has recently been clearly seen in the reaction induced by the radioactive, very weakly bound, halo nucleus  ${}^6\text{He}$  on a  ${}^{238}\text{U}$  target [25]. Our findings have mostly been obtained from the results extracted from elastic scattering data analyses for the lowest energies of four systems. Clearly more work is required to further our understanding of the BTA and its connection with the hindrance of complete fusion of both weakly bound,

stable, nuclei and more so of radioactive nuclei.

### Acknowledgments

This work was partially supported by Financiadora de Estudos e Projetos (FINEP), Fundação de Amparo à Pesquisa do Estado de São Paulo (FAPESP), Fundação de Amparo à Pesquisa do Estado do Rio de Janeiro (FAPERJ), Instituto de Milênio de Informação Quântica (MCT), and Conselho Nacional de Desenvolvimento Científico e Tecnológico (CNPq).

- 
- [1] M. E. Brandan and G. R. Satchler, *Phys. Rep.* **285**, 143 (1997).
  - [2] G. R. Satchler, *Phys. Rep.* **199**, 147 (1991).
  - [3] C. Signorini, *Europ. Phys. Journal* **A13**, 129 (2002).
  - [4] A. M. M. Maciel et al., *Phys. Rev.* **C59**, 2103 (1999).
  - [5] W. Y. So, S. W. Hong, B. T. Kim and T. Udagawa, *Phys. Rev.* **C69**, 064606 (2004).
  - [6] C. Tenreiro et al., *Phys. Rev.* **C53**, 2870 (1996).
  - [7] L. C. Chamon, D. Pereira, M. S. Hussein, M. A. Candido Ribeiro and D. Galetti, *Phys. Rev. Lett.* **79**, 5218 (1997).
  - [8] L. C. Chamon, D. Pereira and M. S. Hussein, *Phys. Rev.* **C58**, 576 (1998).
  - [9] L. C. Chamon et al., *Phys. Rev.* **C66**, 014610 (2002).
  - [10] M. A. G. Alvarez et al., *Nucl. Phys.* **A723**, 93 (2003).
  - [11] M. A. Candido Ribeiro, L. C. Chamon, D. Pereira, M. S. Hussein and D. Galetti, *Phys. Rev. Lett.* **78**, 3270 (1997).
  - [12] D. T. Khoa, G. R. Satchler and W. von Oertzen, *Phys. Rev.* **C56**, 954 (1997).
  - [13] A. Lepine-Szily, M. S. Hussein, R. Lichtenthaler, J. Cseh and G. Levai, *Phys. Rev. Lett.* **82**, 3972 (1999).
  - [14] B. V. Carlson, T. Frederico, M. S. Hussein, H. Esbensen and S. Landowne, *Phys. Rev.* **C41**, 933 (1990).
  - [15] A. B. Balantekin and N. Takigawa, *Rev. Mod. Phys.* **70**, 77 (1998).
  - [16] M. S. Hussein, M. P. Pato, L. F. Canto and R. Donangelo, *Phys. Rev.* **C46**, 377 (1992).
  - [17] M. S. Hussein, M. P. Pato, L. F. Canto and R. Donangelo, *Phys. Rev.* **C47**, 2398 (1993).
  - [18] N. Takigawa, M. Kuratani and H. Sagawa, *Phys. Rev.* **C47**, R2470 (1993).
  - [19] M. Dasgupta et al., *Phys. Rev. Lett.* **82**, 1395 (1999).
  - [20] M. Dasgupta et al., *Phys. Rev.* **C66**, 041602(R) (2002).
  - [21] M. Dasgupta et al., *Phys. Rev.* **C70**, 024606 (2004).
  - [22] V. Tripathi et al., *Phys. Rev. Lett.* **88**, 172701 (2002).
  - [23] S. B. Moraes et al., *Phys. Rev.* **C61**, 64608 (2000).
  - [24] R. S. Mackintosh and N. Keeley, *Phys. Rev.* **C70**, 024604 (2004).
  - [25] R. Raabe et al., *Nature* **431**, 823 (2004).

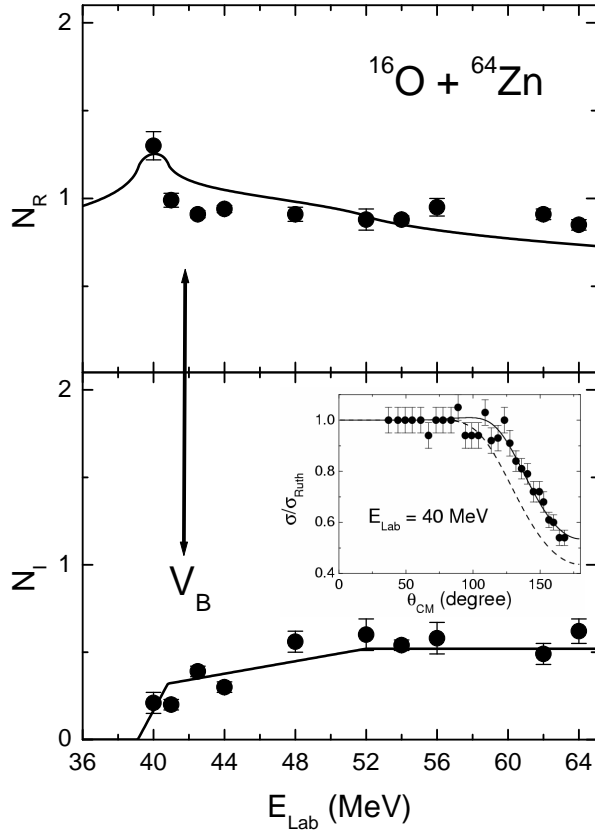


FIG. 1: Energy dependence of the normalization factors  $N_R$  and  $N_I$  of the SP potential for the  $^{16}\text{O} + ^{64}\text{Zn}$  system. The lines represent possible behaviors of  $N_R$  and  $N_I$  that are compatible with the dispersion relation, where  $N_R$  was obtained through Eqs. 4-9 with  $N_{R0}=1.2$ . The approximate position of the barrier height ( $V_B$ ) is indicated in the figure. The elastic scattering angular distribution for the lowest energy is presented in the inset. The dashed line represents predictions with the standard values  $N_R=1$  and  $N_I=0.78$ , while the solid line corresponds to the results obtained with the best  $N_R$  and  $N_I$  values for this energy.

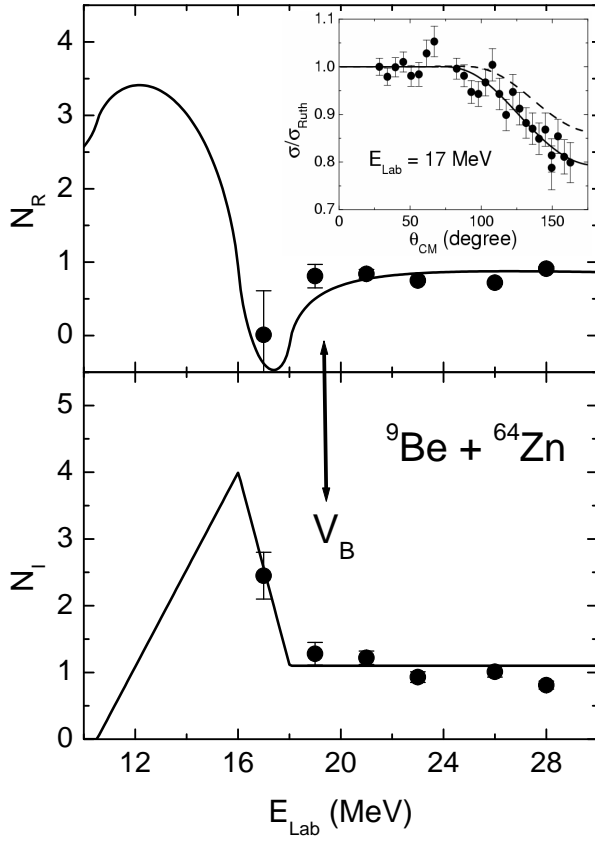


FIG. 2: The same as Figure 1, for the  ${}^9\text{Be} + {}^{64}\text{Zn}$  system ( $N_{R0}=0.9$ ).

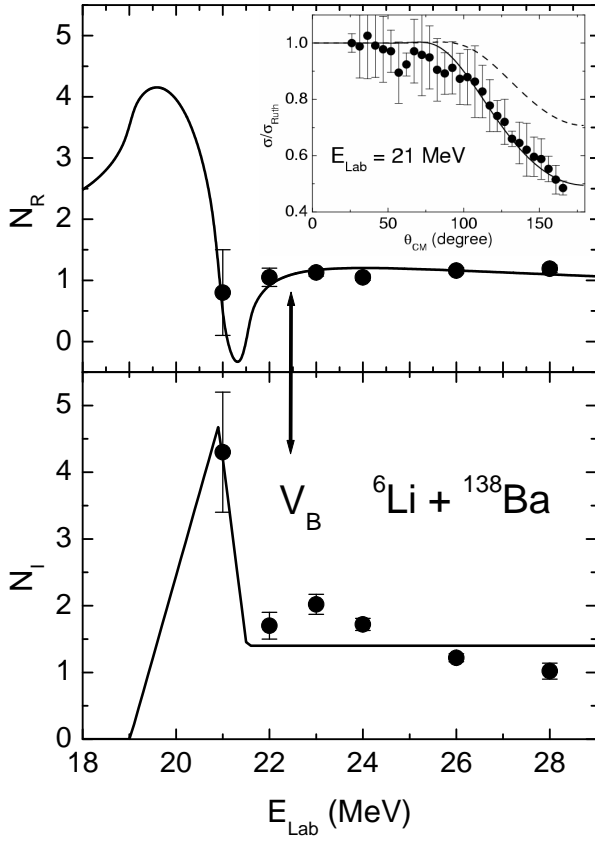


FIG. 3: The same as Figure 1, for the  ${}^6\text{Li} + {}^{138}\text{Ba}$  system ( $N_{R0}=1.15$ ).

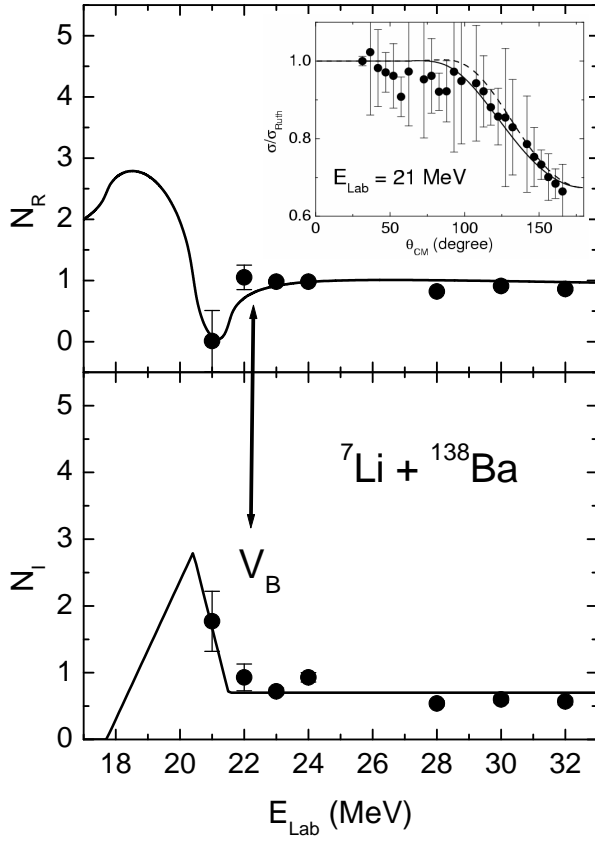


FIG. 4: The same as Figure 1, for the  ${}^7\text{Li} + {}^{138}\text{Ba}$  system ( $N_{R0}=1.05$ ).